1246 | https://doi.org/10.3311/PPci.21908
Creative Commons Attribution

Periodica Polytechnica Civil Engineering, 67(4), pp. 1246–1263, 2023

Optimization of the Engineering Properties of Cement Concrete Containing Gravel and Waste Rock Using Dense Packing and Response Surface Methodology

Nguyen Van Minh[1*], Van Minh Nguyen[2*], Nguyen Viet Anh[2]

[1] Faculty of Civil Engineering, University of Transport Technology, 54 Trieu Khuc, Thanh Xuan, Hanoi 100000, Vietnam
[2] Institute of Technology, 3 Cau Vong, Duc Thang, Bac Tu Liem, Hanoi 100000, Vietnam
[*] Corresponding author, e-mail: minhnv@utt.edu.vn, chinhnhan88@gmail.com

Received: 21 January 2023, Accepted: 28 June 2023, Published online: 26 July 2023

Abstract

This study introduces a novel methodology for optimizing the distribution of aggregate particles in concrete. Utilizing locally available materials like gravel and waste rock is explored as a sustainable alternative to conventional materials like mountain rock and river sand, which are depleting. Determining the maximum bulk density involves an efficient process of gradually adding different particle sizes of gravel and waste rock to the mixture. The vibrational compaction of the container aids in identifying the optimally combined percentages of these aggregates. Besides, the study also addresses the issue of porosity in concrete. The response surface methodology is employed to optimize the mixture proportions for concrete, considering important factors such as workability, compressive strength, flexural strength, and elastic modulus. This response surface methodology allows for the development of mathematical models that aid in determining the optimal mix ratios. By exploiting the potential of gravel and waste rock, this study aims to procedure cement concrete containing gravels and waste rock (WR) with required compressive strength from 30 MPa to 35 MPa based on reasonable aggregate particle distribution in combination with response surface methodology (RSM) and minimize the disposal of non-biodegradable waste, thereby reducing the environmental pollution. Additionally, utilizing locally available materials helps to effectively use the region's resources for concrete production, promoting sustainability and reducing dependency on scarce resources. The proposed method presents a promising approach to optimizing aggregate distribution in concrete while considering the environmental and resource constraints specific to the Northwest region of Vietnam.

Keywords

cement concrete, gravel aggregate, waste rock, response surface methodology (RSM), engineering properties

1 Introduction

The minor use of aggregates sourced from mountainous areas and riverbeds is essential to ensure sustainable and environmentally friendly construction [1]. Add to that pledge from Vietnam to achieve zero CO_2 emissions by 2050 at the climate change conference COP26 in Glasgow. Therefore, using environmentally friendly building materials and recycling industrial waste have been fascinating and actively promoted research areas. Aggregates typically account for 80–85% of the weight in cement concrete, while cement accounts for 8–15%, which can affect the engineering properties of cement concrete [2]. The strength of cement concrete can impact by various factors, including the structure, shape, and properties of the aggregate [3]. In addition, the W/C ratio, the cement and aggregate (C/A) ratio, and the proportion of other material components all affect the properties of cement concrete [4].

Gravel is a naturally formed material caused by physical and chemical processes within the crust of Earth. Classification of gravel can base on shape, with three predominant types identified: round, elongated, and irregular aggregates [5]. According to Saxena and Pofale [6], replacing 80% of the crushed coarse aggregate (rock) with gravel resulted in the height compressive strength, tensile strength, and flexural strength. However, replacement up to 100% led to a decrease in these strength properties [6]. Previous studies utilized gravel, pebbles, or round stones in concrete construction led to a reduction of approximately 4–5% in the cement volume per 1m3 of concrete compared to other aggregates [7]. Therefore, the origin and shape of the gravel affected the mechanical behavior of cement concrete. Properly sized gravel contributes to the format of a rigid framework within, thereby mitigating

Cite this article as: Nguyen V. M., Van Minh, N., Nguyen V. A. "Optimization of the Engineering Properties of Cement Concrete Containing Gravel and Waste Rock Using Dense Packing and Response Surface Methodology", Periodica Polytechnica Civil Engineering, 67(4), pp. 1246–1263, 2023. https://doi.org/10.3311/PPci.21908

shrinkage in concrete [8, 9]. Shrinkage deformation is affected not only by the quality of the gravel but also by its content [10]. The best gravel particle size combination will create a concrete mixture with the minimum porosity and significantly reduce the amount of cement used (the most expensive material price in concrete) while maintaining the engineering properties of concrete [11].

In response to the depletion of traditional materials, like river sand, in concrete production, there is a pressing need to explore alternative sources such as waste or recycled materials as substitutes for river sand. Waste sand can use to manufacture high-quality concrete [12] and self-compacting concrete [13]. However, compared with natural sand, previous studies have listed some differences between sand the waste rock as its more angular grain shape, coarser grain size, and higher adsorption capacity than river sand [14, 15]. The amount of WR material obtained from stone block processing requires storage space. Using WR as an alternative to natural sand for concrete production is a promising direction that can reduce recycling costs and increase the efficiency of using aggregate materials in concrete. However, the overall picture showing the use of WR as a fine aggregate for concrete is still incomplete, unclear, and immediately inapplicable. Thus far, research has often focused on the problem of reusing WR from processing granite or limestone instead of river sand [16]. Besides, some types of WR derived from quartz stone processing could not evaluate. Therefore, this study initially investigates quartz WR in concrete fabrication for infrastructure construction, with required compressive strength of 30–35 MPa based on using the statistical surface method to optimize and prioritize the engineering properties of concrete. The application of response surface methodology allows the reduction of the required experiments to the necessary extent while concurrently providing a substantial amount of valuable information [17]. The response surface methodology (RSM) currently used to solve technical problems has the following advantages: The experimental process used a minor number of experiments, and the calculation and design process was simple and accurate [18]. RSM proves to be an excellent technique for identifying relationships between the investigating value and the influencing variables with optimizing target value when it was a function influenced by multiple variables [19]. When determining the optimal mixture proportions of the concrete using gravel and WR, RSM can improve the engineering properties of fresh and hardened concrete. RSM can resolve the optimum zone for concrete mix slump, compressive and flexural strengths of cement concrete, reducing laboratory testing time and saving materials while still achieving the design intensity [20]. A literature review reveals that some research investigated cement, mortar, and cement concrete using RSM [21–23]. But the application for concrete containing gravel and WR has not yet been considered.

The research process in this work can divide into two stages. The first phase focused on optimizing the process of distributing aggregate particles by size using the dense packing method. The second phase involved using RSM to calculate the concrete mix proportions and optimize the W/C and mortar residual coefficient α variables according to the engineering properties of concrete.

Northwest encompasses a vast territory characterized by high altitude, steep slopes, and extensive topographical dissection. The Northwest has geographical coordinates: latitude 20°47' N to 22°48' N; longitude 102°09' E to 105°52' E. The Northwest topography takes the form of a medium-high mountainous terrain (the absolute height is from 820 m to 1500 m), folds, and eroded blocks, including high mountain ranges with steep slopes running in the Northwest - Southeast direction, alternating with narrow valleys running along rivers and streams (Fig. 1). The streams are short and steep, with many rapids and the stream bed is full of rocks and gravel.

The transportation of aggregates from other regions to the Northwest was a significant challenge due to the complexity of the topography, in addition to the primary road system being dirt roads. Therefore, the study of using local materials and waste materials to produce concrete with required compressive strength from 30 MPa to 35 MPa was a pressing task that was also the focus of this article.

Fig. 1 Typical topography of the Northwest region of Vietnam

Waste rock from quartz stone processing has been concentrated in Son La province in a storage yard with reserves of up to 0.8 billion m^3. In terms of cement materials, the Northwest has several cement plants (CP), including the Thai Nguyen CP, which has a capacity of 1.4 million tons per year; the Song Thao CP, the Dong Banh CP; the Son La CP; the Tuyen Quang CP; the Trung Son CP and the Yen Binh CP – 0.9 million tons per year (in each plant).

This study presents a novel methodology for optimizing the distribution of aggregate particles in concrete while considering the utilization of locally available materials in the Northwest region of Vietnam (waste rock, gravel) as alternatives to conventional materials (mountain rock, river sand) that are depleting. The maximum bulk density is determined by gradually adding different particle sizes and vibrating the container to identify the optimally combined percentages. The study also addresses porosity by incorporating aggregates of specific sizes. The mixture proportions for concrete are optimized using mathematical models and statistical analyses, considering factors like workability, compressive strength, flexural strength, and elastic modulus. By harnessing the potential of gravel and waste rock, the study aims to minimize non-biodegradable waste disposal, reduce environmental pollution, and effectively utilize local resources for concrete production of compressive strength 30–35 MPa.

2 Research method and material

2.1 Test techniques

The cement, aggregate, and concrete specimens can test for the following:

a. For cement: specific gravity ASTM C188 [24]; amount of water required ASTM C187 [25]; specific surface (Blain method) ASTM C204 [26]; time of setting ASTM C191 [27]; compressive strength ASTM C109 [28].
b. For aggregate: Sieve analysis ASTM C136 [29]; specific gravity and water absorption ASTM C127 [30] and ASTM C128 [31]; bulk density and voids in aggregate ASTM C29 [32]; Los Angeles abrasion ASTM C131 [33]; Micro-Deval abrasion ASTM D6928 [34]; potential alkali reactivity (mortar-bar method) ASTM C1260 [35].
c. For concrete: Making and curing specimens ASTM C192 [36]; slump ASTM C143 [37]; compressive strength ASTM C39 [38]; flexural strength ASTM C78 [39]; elastic modulus ASTM C469 [40].
d. The porosity of aggregate mixtures was calculated according to the Eq. (1):

$$Void = \left(1 - \frac{\rho_0}{\rho_a}\right) \times 100\%, \tag{1}$$

where: ρ_0 - bulk density of aggregate; ρ_a - apparent density of aggregate.

The determination of ρ_0 and ρ_a by conventional test methods for gravel and sand is unsuitable because the aggregate mixture has a distribution of aggregates with a particle size of 19–0.15. In this study, the bulk and apparent density can determine as follows: pour the aggregate mixture into a graduated iron barrel, record the volume of aggregate mixture V_1 (liter), and the weight of the aggregate mixture m_1 (kg). Then pour the aggregate mixture into the iron barrel with the water level at V_2 (liters), and record the water rising for the aggregate mixture to displace the place of V_3 (liters).

The bulk density of the mixture can determine by Eq. (2), and the apparent density can determine by Eq. (3):

$$\rho_0 = \frac{m}{V_1}, \tag{2}$$

$$\rho_a = \frac{m}{V_3 - V_2}. \tag{3}$$

2.2 Experimental material

2.2.1 Cement

In the Northwest of Vietnam, the primary type of cement is Portland mixed (PCB). For this study, the binder of choice was PCB40 cement. The mechanical properties of the cement are given in Table 1, the chemical composition of the cement is given in Table 2, and the mineral composition is given in Table 3.

Table 1 Mechanical and physical properties of the PCB40 cement

Property	Unit	Result
Apparent density	g/cm^3	3.12
Amount of water required	%	28.5
Fineness (Blain method)	cm^2/g	3760
Time of setting	Minute	120 ÷ 215
Compressive strength at 28 days	MPa	40.78
Flexural strength at 28 days	MPa	6.12

Table 2 Chemical composition of the PCB40 cement

SiO_2	Al_2O_3	Fe_2O_3	CaO	MgO	SO_3	Na_2O	K_2O	CaO free
22.41	3.98	2.87	58.97	1.02	2.18	0.42	0.84	2.86

Table 3 Mineral composition of the PCB40 cement

C_3S	C_2S	C_3A	C_4AF	Mineral additives
51	25	5.1	10	8.9

2.2.2 Aggregate

The gravel used in this study was a type of mechanical sedimentary rock in the form of individual grains, the size of which ranges from 4.75 to 19 mm. Based on the visual assessment of particle shape published by Powers [41], the gravel used in this study has rounded and sub-rounded forms. For surface texture, upon tactile contact, gravels elicit a sensation of irregularity and roughness (Fig. 2). After being extracted in nature, gravel can be classified based on its particle sizes. The mechanical and physical properties of the aggregate (gravel and waste rock) are shown in Table 4.

The requirements for the particle size distribution of gravel can follow the standard ASTM C33 [42]. The granulometric composition of gravel is shown in Fig. 3.

The waste rock used in the study has some characteristics, such as low sphericity, mainly flat and long particles (see Fig. 2 and Fig. 4). Requirements for the granulometric composition of waste rock particles are given in the standard ASTM C33 [42]. The size distribution of waste rock particles is shown in Fig. 3. Therefore, waste rock concrete frequently has poor workability and water separation. However, waste rock has a rough, sharp surface, free of dirt and organic impurities. The mineral composition of the waste rock material was analyzed using the X-ray diffraction method. The results of the analysis are shown in Fig. 5 and Table 5.

Observing the waste rock surface, it is evident that the rock has a gray color and block structure, wherein the crystals are visible and characterized by well-defined faces, which have no pores. The X-ray diffraction pattern shows that the waste rock material exhibits a distinct crystalline structure. According to the results of the mineral composition analysis, it can find that the content of quartz is 32–36%, feldspar 38–46%, and mica 4–7%.

In terms of alkali silicon reaction (ASR), the mechanism of this reaction is as follows: the OH^- ion combines with K_2O, and Na_2O from cement, water, and other sources, the Na^+, K^+ cations and OH^- anion accumulates to increase the pH, leading to a reaction in the aggregate, this time depending on the concentration of OH^- ion, the W/C ratio, the degree of reactivity, and the form of various gels and sols. SiO_2 always dissolves in a high-pH solution.

Fig. 2 Gravel and waste rock used in the study

Table 4 Mechanical and physical properties of the gravel

Property	Gravel	Waste rock	Unit
Apparent density	2.70	2.72	g/cm^3
Bulk density	1562	1710	kg/m^3
Los Angeles	12.1	-	%
Micro Deval	-	12.8	%
Surface moisture	0.41	0.58	%
Absorption	1.9	0.7	%
Fineness modulus	-	3.3	

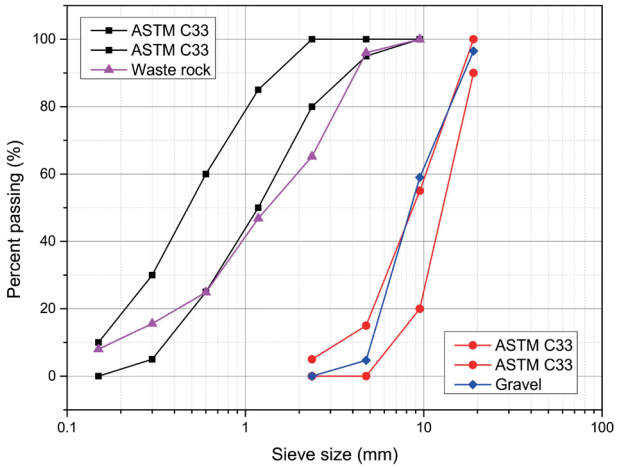

Fig. 3 Particle size distribution of the gravel and waste rock

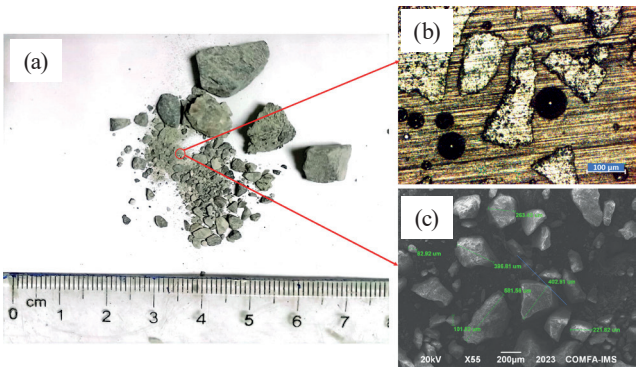

Fig. 4 Morphological characteristics of waste rock

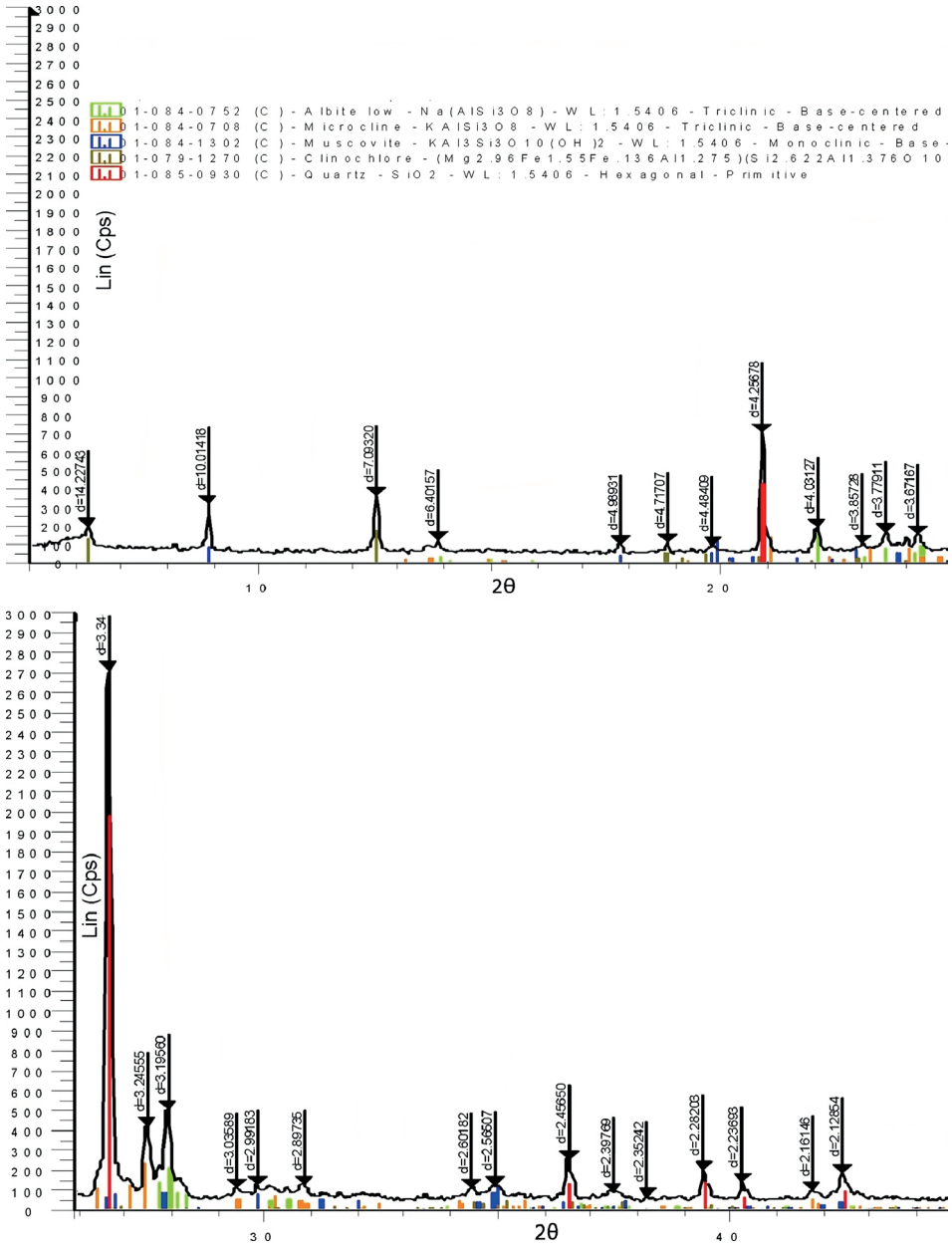

Fig. 5 X-ray diffraction pattern of the waste rock material

Table 5 Content and type of minerals of waste rock

Minerals	Content, %	Notice
Quartz	32–36	SiO_2
Microcline	16–20	$KAlSi_3O_8$
Albite	22–26	$Na(AlSi_3O_8)$
Clinochlore	10–15	$(Mg_5Al)(AlSi_3)O_{10}(OH)_8$
Muscovite	4–7	$KAl_2(AlSi_3O_{10})(F,OH)_2$

The initial product regularly consists of non-blooming calcium silica gels. It is similar to the C-H-S chain present in cementitious materials. At this time, if the solution (mortar) has an excess of SiO_2, it will then act from the surface to the inside of the core of the aggregate, creating potassium silica. This product will swell in volume with water, causing damage to the aggregate skeleton and thereby indirectly destroying the cement concrete structure. The method "deformation of mortar bar" can be employed to assess the ASR of the waste rock [35]. Experimental results are presented in Table 6.

Table 6 Deformation of mortar bar due to ASR reaction

Deformation of mortar bar due to the influence of ASR when using waste rock, %						
1 day	30 days	60 days	90 days	120 days	150 days	180 days
0	0.021	0.035	0.043	0.056	0.061	0.068

The results show that the deformation of the mortar bar increases with time, but the rate of rise is not significant. The deformation of mortar bars at 30 days of age reached 0.021%, and the deformation at 180 days continued to increase and reached 0.068%. These values are below the required threshold of 0.1% [35]. The assessment indicated that the waste rock sample exhibits a low susceptibility to ASR.

2.3 Optimization of the distribution of aggregate particles by size

The particle content can determine according to ASTM C136 [29]. Gravel volume saturation can achieve when the particle size distribution is optimal. This saturation means the maximum volume. The determination of the highest volumetric, which indicates the degree of compactness of the aggregate, can be carried out in its bulk state and sometimes in its compacted regime. For this study, the gravel container vibrated on the vibrating table. The study demonstrated a significant increase in the volume of gravel, ranging from 20% to 35% when subjected to vibrations. However, it is difficult to determine the maximum bulk density of the aggregate mixture by particle size distribution. To determine the maximum bulk density of the aggregate mix, one can use the method as follows: in an iron barrel with a volume of 2 liters, add rock aggregate of the largest size, divided into third times: for the first time, put it into 1/3 of the barrel, vibrate for 60 seconds; for the second time, put on 2/3 barrels, vibration for 60 seconds; for the third time, fill the barrel and finish vibration for 60 seconds. Align the surface and calculate the bulk density of the particle grade. Next, we mix the second grade with the first (with such a mass to fill the voids of the first grade) and proceed in turn, as described above. By doing this down to the final particle grade, it was possible to obtain the maximum bulk density of the aggregate mixture.

The aggregates, after sieving, have the following sizes: 19–9.5 (A_1), 9.5–4.75 (A_2), 4.75–2.36 (A_3), 2.36–1.18 (A_4), 1.18–0.6 (A_5), 0.6–0.3 (A_6), và 0.3–0.15 (A_7). The experimental determination of the optimal aggregate mix, represented by the beta value, is illustrated in Fig. 6.

Sieve the aggregates into separate particles, then determine the bulk density of each particle grade (according to size), the results are presented in Table 7.

Based on the suggested method, gravel with particle sizes 19–9.5 and 9.5–4.75 was combined in different proportions to obtain the aggregate mixture with the maximum bulk density. The results are shown in Fig. 7. The highest bulk density results revealed that the optimal combination of particle sizes 19–9.5 and 9.5–4.75 was achieved with proportions of 61.44% and 38.56%, respectively.

Similarly, to explore the optimal percentage combination for achieving the maximum bulk density, additional particle sizes 4.75–2.36, 2.36–1.18, 1.18–0.6, 0.6–0.3, and 0.3–0.15 will be sequentially added and evaluated. The results are shown in Table 8.

By mixing aggregates of different sizes, the porosity value range from 45.42% to 30.63% in the resulting mixture. The porosity of aggregates without particle size

Table 7 Bulk density of each particle grade

Bulk density of each particle grade (according to size in mm), kg/m^3						
19–9.5	9.5–4.75	4.75–2.36	2.63–1.18	1.18–0.6	0.6–0.3	0.3–0.15
1447	1422	1403	1387	1371	1360	1353

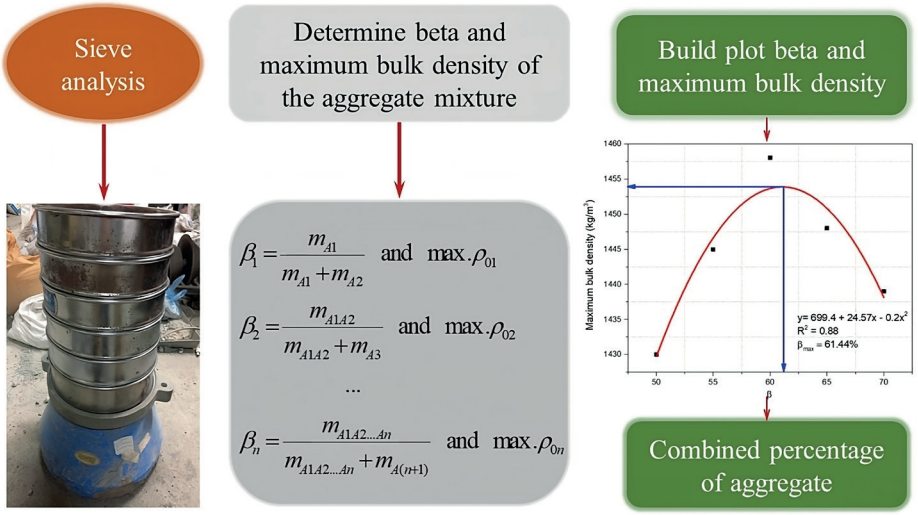

Fig. 6 Procedure for determining the optimal percentage of aggregates

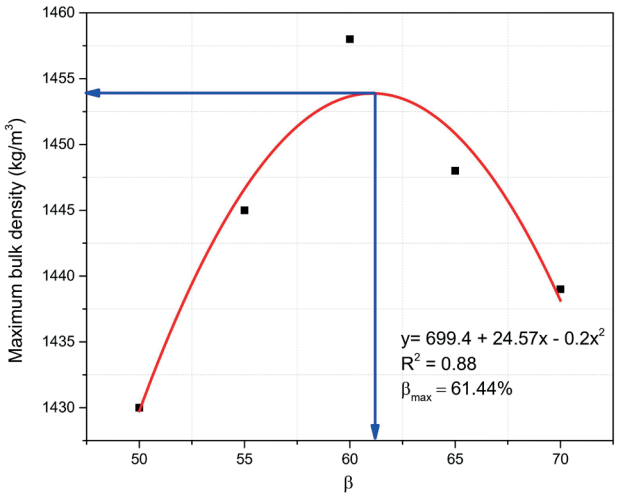

Fig. 7 Combined percentage of particle sizes

4.75–0.015 mm was above 42%, indicating a substantial impact of this particle size on reducing porosity. For a single aggregate size, porosity can be reduced from 2% to 3% when adding aggregates with a particle size of 4.75–0.15 mm. The combination of 19–4.75 mm showed minimal changes in porosity. Therefore, adding 4.75–0.15 mm of WR could be deemed suitable for effectively adjusting the porosity of the aggregate mix.

2.4 Optimization of mixture proportions of concrete

The Bolomei-Skramtaev method, in combination with the RSM, can be exploited to determine the proportions of the concrete mixture. In the laboratory, RSM is a widely utilized approach for optimizing mix ratios in various applications [43]. Based on the experimental results, set up mathematical models to show the relationship between the object of study and the influencing factors. It gives innovative measures aimed at optimizing the strength characteristics of cement concrete.

Component materials for making concrete can calculate according to the following steps:

- *Step 1*: The selection of the slump for the concrete mix depends on the type of structure and construction conditions, employing the compact method;
- *Step 2*: Determine the amount of mixing water (W), in which the amount of mixing water is selected based on the required slump determined in Step 1, along with the criteria of the materials used for the concrete mix;
- *Step 3*: Determine the cement/water ratio (C/W) by Eq. (4):

$$\frac{C}{W} = \frac{R_b}{A \cdot R_x} + 0.5 . \quad (4)$$

- *Step 4*: Determine the mass of cement (C) by Eq. (5):

$$C = W \frac{C}{W} . \quad (5)$$

- *Step 5*: Determine the mass of the gravel (G) by Eq. (6):

$$G = \frac{\rho_{oG}}{r \cdot (\alpha - 1) + 1} . \quad (6)$$

- *Step 6*: Determine the mass of the waste rock (WR) by Eq. (7):

$$WR = \left(1000 - \frac{C}{\rho_{aC}} - W - \frac{G}{\rho_{aG}}\right)\rho_{aWR} , \quad (7)$$

where: R_b - Compressive strength of concrete, is taken by the required concrete compressive strength multiplied by safety factor 1.1 for automatic batching plant and 1.15 for manual batching plant, MPa; R_x - Compressive strength of cement, MPa; A - Material quality factor; r - Porosity between aggregate particles, %; ρ_{oG} - Bulk density of gravel, g/cm^3; ρ_{aG} - Apparent density of gravel, g/cm^3; ρ_{aC} - Apparent density of cement, g/cm^3; ρ_{aWR} - Apparent density of waste rock, g/cm^3; α – Mortar residual coefficient.

For cementitious concrete, some of the main factors affecting the quality of concrete are W/C and mortar residual coefficient [4]. Fabricated concrete has the required strength of 30 MPa to 35 MPa, applying Eq. (4) has found the C/W ratio from 0.39 to 0.44 (aggregate quality factor A = 0.47). Reaching the required workability in fresh con-

Table 8 Combination of particle grades

Combined ratio of particle grades, %							Bulk density, kg/m^3	Porosity, %
19–9.5	9.5–4.75	4.75–2.36	2.36–1.18	1.18–0.6	0.6–0.3	0.3–0.15		
61.44	38.56	0	0	0	0	0	1454	45.42
	63.62	36.38	0	0	0	0	1521	42.91
		65.53	34.47	0	0	0	1619	39.23
			67.25	32.75	0	0	1708	35.89
				70.84	29.16	0	1786	32.96
					71.75	28.25	1848	30.63

crete mix relies on ensuring that the cement paste effectively encapsulates the aggregate particles, as indicated by the residual mortar coefficient α. The sand derived from WR has a fineness modulus of 3.3, with preliminary experimental results for α ranging from 1.55 to 1.94. The ranges of the variables W/C and α are presented in Table 9. The studied concrete mix components are presented in Table 10.

The independent variables were the W/C and α. They are encoded using the variables X_1 and X_2, respectively. The process variables can be optimized using a central composite design (CCD) involving 13 runs. The experimental data prepared for quadratic polynomial models, depicting the relationship between the independent variables and the concrete mixture's workability (R_1), compressive strength (R_2), flexural strength (R_3), and elastic modulus (R_4), were as follows Eq. (8):

Table 9 Factor ranges in terms of W/C and α

Variables	Symbol	Coded levels		
		Low	Medium	High
		-1	0	+1
W/C	A	0.39	0.42	0.44
α	B	1.55	1.75	1.94

$$R_n = b_0 + \sum_{i=1}^{2} b_i X_i + \sum_{i=1}^{2} b_{ii} X_i^2 + \sum_{i=1}^{2} b_i j X_i X_j , \quad (8)$$

where R_n (n = 1÷3) represents the functions R_1, R_c, and R_3; b_0 is the empirical regression coefficients; b_i, b_{ij}, and b_{ii} are interaction, linear and quadratic coefficients, respectively; X_i and X_j are the independent variables.

3 Results and discussion

3.1 Suitability and check the acceptability of the model

The purpose of RSM is to find a way to optimize the input data in the investigational area to obtain the desired optimized experimental output data. The sequence of steps for the RSM analysis is shown in Fig. 8 [18].

The ranges and levels of the variables A (W/C ratio), B (residual mortar coefficient α), and experimental results are presented in their coding form in Table 11.

In this study, F-test, T-test, and R-square (R^2) in analysis (ANOVA) were used to assess the goodness of fit of the selected model and remove variables that did not strongly influence the model [22]. In Table 12, appropriate models can suggest slump, compressive, flexural strength, and elastic modulus.

Table 10 Mass of component materials for 1 m^3 of concrete

Std	Run	W/C	α	Cement, kg	Water, kg	Gravel, kg		Waste rock, kg				
						19-9.5	9.5–4.75	4.75–2.36	2.36–1.18	1.18–0.6	0.6–0.3	0.3–0.15
1	12	0.39	1.55	462	180	779	489	123	65	92	115	155
2	11	0.44	1.55	409	180	779	489	133	70	99	125	168
3	6	0.39	1.94	462	180	688	431	157	82	117	146	198
4	1	0.44	1.94	409	180	688	431	167	88	124	156	211
5	13	0.38	1.75	474	180	729	458	139	73	103	130	175
6	7	0.45	1.75	400	180	729	458	154	81	114	144	194
7	8	0.42	1.47	429	180	801	503	122	64	90	114	153
8	4	0.42	2.02	429	180	671	421	169	89	126	158	214
9	10	0.42	1.75	429	180	729	458	148	78	110	138	187
10	2	0.42	1.75	429	180	729	458	148	78	110	138	187
11	3	0.42	1.75	429	180	729	458	148	78	110	138	187
12	9	0.42	1.75	429	180	729	458	148	78	110	138	187
13	5	0.42	1.75	429	180	729	458	148	78	110	138	187

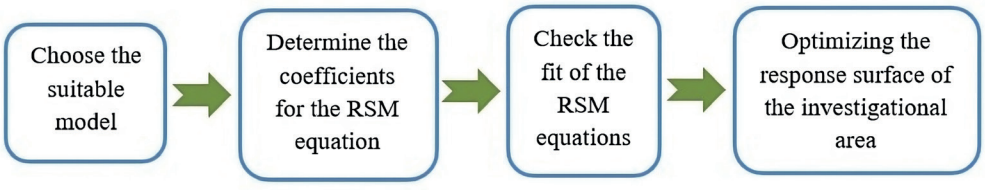

Fig. 8 Basic sequence of an RSM

Table 11 The independent variables (A, B) and experimental results of the slump (R_1), compressive strength (R_2), flexural strength (R_3), and elastic modulus (R_4)

Std	Run	Ratio water/cement (A)	Residual mortar coefficient (B)	Slump (R_1), cm	Compressive strength (R_2), MPa	Flexural strength (R_3), MPa	Elastic modulus (R_4), GPa
1	12	0.39 (-1.0)*	1.55 (-1.0)	8.5	29.1	2.9	31.765
2	11	0.44 (1.0)	1.55 (-1.0)	9.0	26.2	2.6	24.659
3	6	0.39 (-1.0)	1.94 (1.0)	7.5	33.0	3.4	32.105
4	1	0.44 (1.0)	1.94 (1.0)	8.5	30.0	2.9	28.176
5	13	0.38 (-1.414)	1.75 (0.0)	7.5	35.4	3.3	35.054
6	7	0.45 (1.414)	1.75 (0.0)	9.0	27.6	2.7	27.128
7	8	0.42 (0.0)	1.47 (1.414)	9.5	26.5	2.5	26.061
8	4	0.42 (0.0)	2.02 (-1.414)	8.5	28.6	2.9	31.126
9	10	0.42 (0.0)	1.75 (0.0)	7.0	36.0	3.6	34.859
10	2	0.42 (0.0)	1.75 (0.0)	8.0	34.3	3.4	33.788
11	3	0.42 (0.0)	1.75 (0.0)	7.5	36.7	3.8	37.106
12	9	0.42 (0.0)	1.75 (0.0)	7.5	35.4	3.5	33.121
13	5	0.42 (0.0)	1.75 (0.0)	8.0	34.6	3.4	31.91

* Values in parentheses were coded variables from actual variables in the experimental design.

Table 12 Proposed model for a slump, compressive, flexural strength, and elastic modulus

	Source	Sequential P-value	Lack of Fit P-value	Adjusted R^2	Predicted R^2	Remark
Slump	Linear	0.0755	0.1442	0.2843	0.0285	
	2FI	0.7139	0.115	0.2172	-0.0621	
	Quadratic	0.0052	0.8042	0.7761	0.6515	Suggested
	Cubic	0.8652	0.4456	0.7041	-0.3588	Aliased
Compressive strength	Linear	0.1980	0.0051	0.1319	-0.2042	
	2FI	0.9898	0.0037	0.0356	-0.6309	
	Quadratic	0.0001	0.2452	0.9053	0.7269	Suggested
	Cubic	0.0954	0.9463	0.9482	0.9646	Aliased
Flexural strength	Linear	0.1983	0.0302	0.1317	-0.1544	
	2FI	0.8113	0.0229	0.0417	-0.4006	
	Quadratic	0.0002	0.8097	0.8849	0.8224	Suggested
	Cubic	0.8763	0.4456	0.8471	0.2979	Aliased
Elastic modulus	Linear	0.0489	0.1313	0.3439	0.1358	
	2FI	0.6283	0.1067	0.2907	-0.2027	
	Quadratic	0.0033	0.8949	0.8214	0.7635	Suggested
	Cubic	0.8176	0.6568	0.7693	0.5239	Aliased

F-test assesses whether the model fits the data or not. The F-value for the "lack of fit" test indicates whether the lack of fit is statistically significant compared to the pure error; a non-significant lack of fit is good.

Conducting T-test helps identify the parameters that have a weak impact on the model; subsequently, those variables are removed from the prediction equation, specifically, comparing the P-value with the significance level in statistics to assess the probability of making an error; if the P-value of any variable is less than 0.05, it indicates that the variable significantly affects the prediction equation and vice versa.

In the regression models, R^2 can calculate as the ratio of the sum of squares of the regression to the total sum of squares. R^2 is usually in the range of 0 to 1. The higher value of R^2 shows a good agreement between the experimental values and the regression equation [18]. However, the use of R^2 to evaluate the correlation between the experiment and the regression equation still has a limitation, there are independent variables and not statistically significant, but the value of R^2 tends to increase and move towards 1. Therefore, to overcome that problem, adjusted R^2 is often used in statistics, in terms of value, adjusted $R^2$is always

smaller than R^2. Adjusted R^2 is not affected by independent variables that exist in the data. The adjusted R^2 and R^2 values should exhibit a strong level of similarity, indicating that the regression equation can apply to the prediction.

In Fig. 9, the perturbation plot in the RSM shows the change in each factor affecting the engineering properties of the concrete as each factor moves away from the reference point (which is a zero-coded level), with all other factors remaining constant at the reference value.

The perturbation plot in Fig. 9 revealed that all factors W/C (coded as A) and α (coded as B) affect the engineering properties of obtained concrete. It observed that an increase in the W/C ratio reduces the compressive, flexural strength, and elastic modulus and increases the slump of the concrete.

In the case of responses, it is suitable to consider normal distributions for effectively comparing the disparity between predicted and actual plots (or between predicted and experimental values). Fig. 10 shows the normal probability distribution of residuals between actual and versus forecast. The data underwent analysis to evaluate the normality of residuals. The plots depicting actual and expected values of concrete engineering properties need to estimate. Through observation, it became evident that the plotted points for the slump, compressive, flexural strength, and elastic modulus exhibited proximity to the fitted distribution line.

Table 13 shows the ANOVA for the slump response model, considering that for the model, the P-value of "lack of fit" is 0.0053, which is smaller than the F-value of the

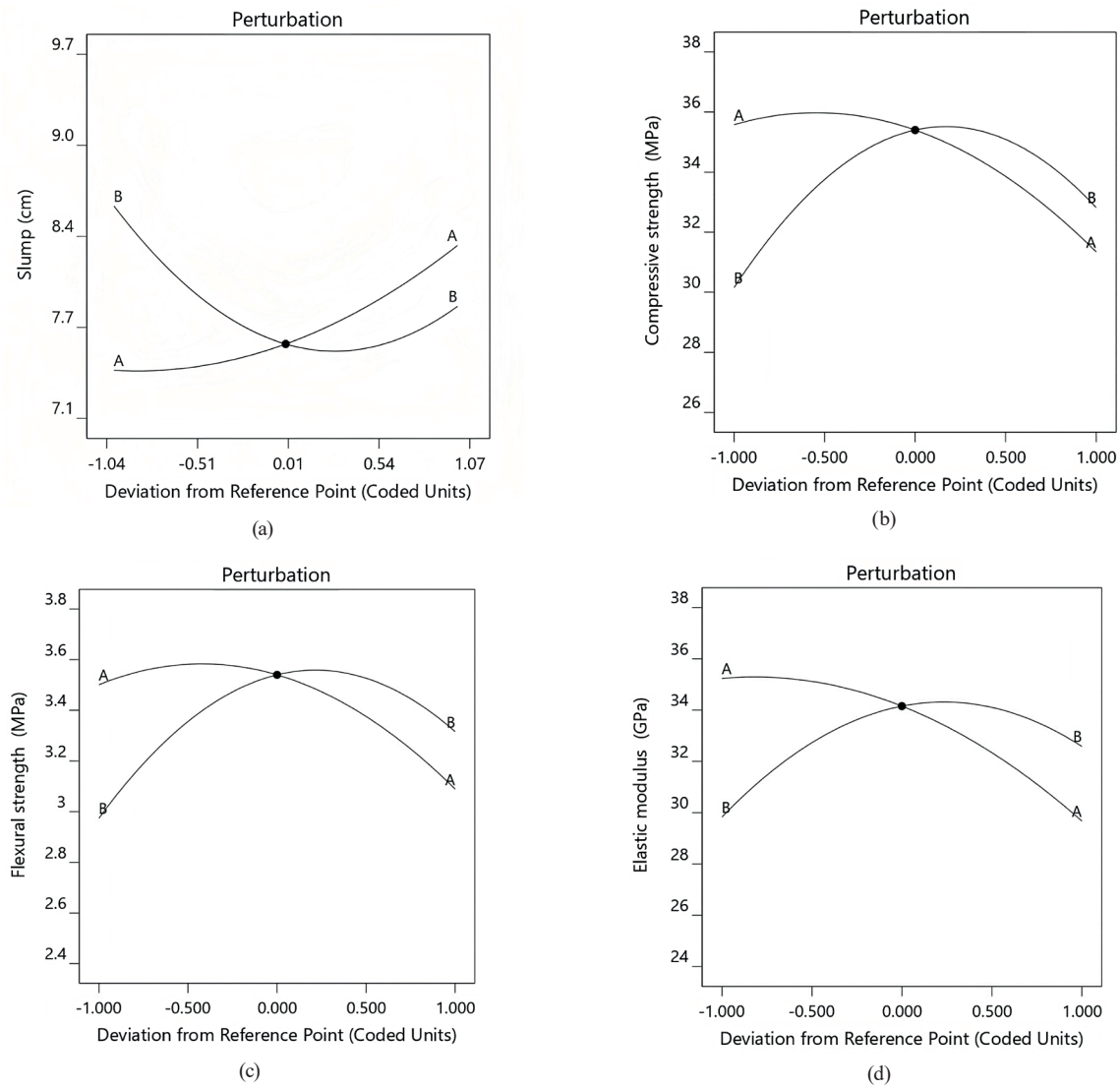

Fig. 9 (a) Perturbation plot for Slump, (b) Perturbation plot Compressive strength, (c) Plot for Flexural strength, (d) Plot for Elastic modulus of the concrete

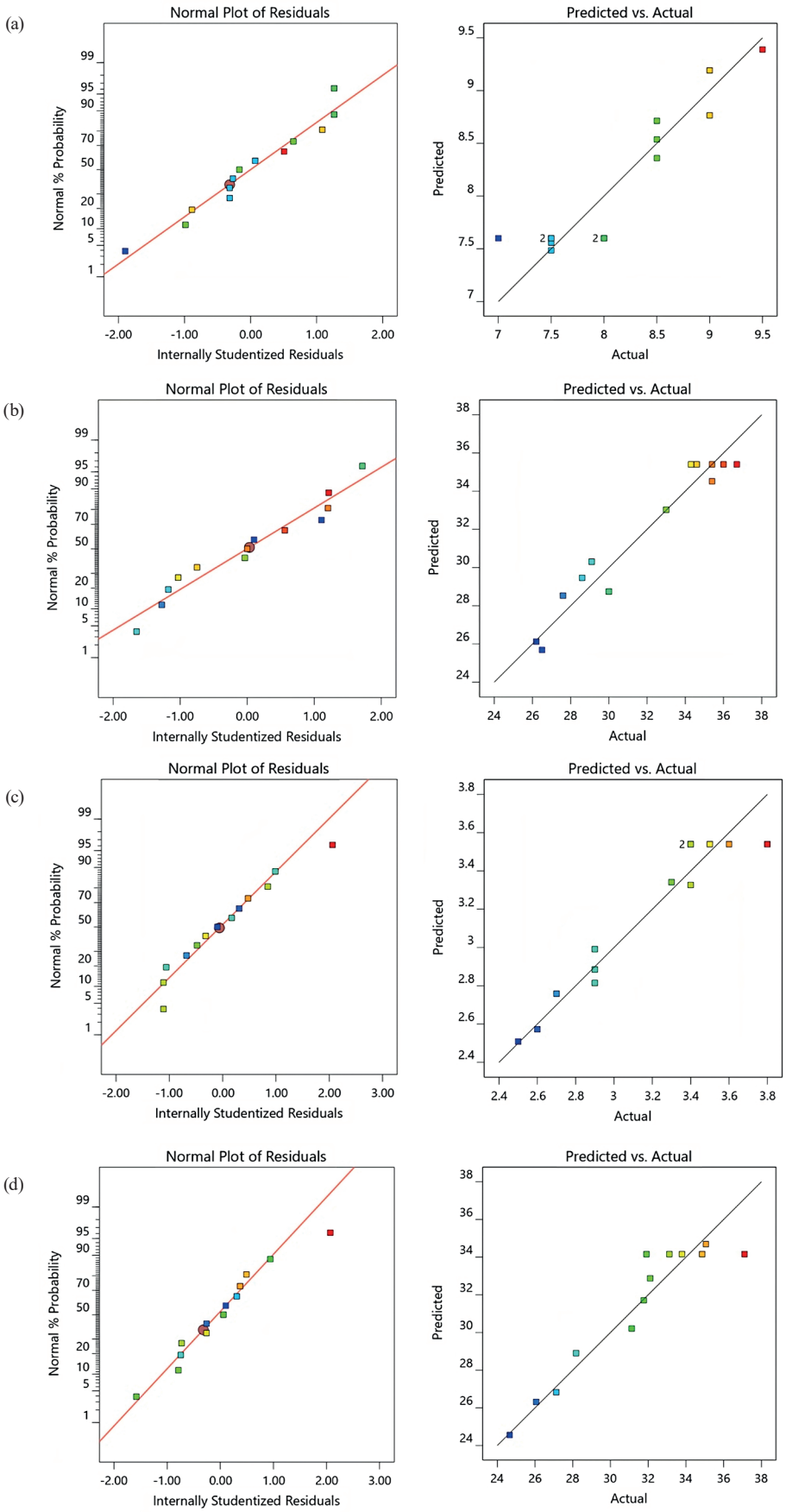

Fig. 10 (a) Standard normal distribution plots for Slump, (b) Standard plots compressive strength, (c) Normal plots distribution for flexural strength, (d) distribution for elastic modulus

model, which is 9.32, which provided finds that the model is suggestive. The R2 value of 0.8694 is close to the R^2-adj value of 0.7761, and both are close to 1, which confirms the reliable agreement between the experimental values and the model. P-values less than 0.05 indicates terms of the model are significant. In this case, W/C, α, α^2 are meaning terms of the model. The coding equation after removing the variables has no effect, Eq. (9):

$$R_1 = 7.6 + 0.4527A - 0.3643B + 0.5375B^2 . \quad (9)$$

Except for W/C*α, $(W/C)^2$, the other variables all influence the slump. The findings indicate a positive correlation between the W/C ratio and the slump property, suggesting that an increase in the W/C ratio is associated with a rise in workability. Surprisingly, the first-order coefficient of α exhibited an inverse relationship with the slump, and the second-order coefficient α^2 demonstrated a direct proportionality to the change in slump property. Each unit increase in α^2 resulted in an average gain of 0.6375 of the slump. The variables W/C, α, and α^2 all had a significant influence on the model. Fig. 11 shows a 3D surface and contour plot of the slump.

Table 13 presents the ANOVA for the compressive strength response model, the P-value "lack of fit" of the model is 0.0003 which is smaller than the F value of the model, which is 23.95, which proves that the model is significant. R^2 value of 0.9448 is close to adjusted R^2 value of 0.9053, which confirms the reliable agreement between the experimental values and the model. The variables affecting compressive strength are W/C, α, $(W/C)^2$, α^2. Values greater than 0.1 indicate terms of the model are not significant; in this case, this is W/C*α. The coding equation for predicting compressive strength (R^2) after removing non-significant variables, Eq. (10):

$$R_2 = 35.4 - 2.12A + 1.33B - 1.94A^2 - 3.91B^2 . \quad (10)$$

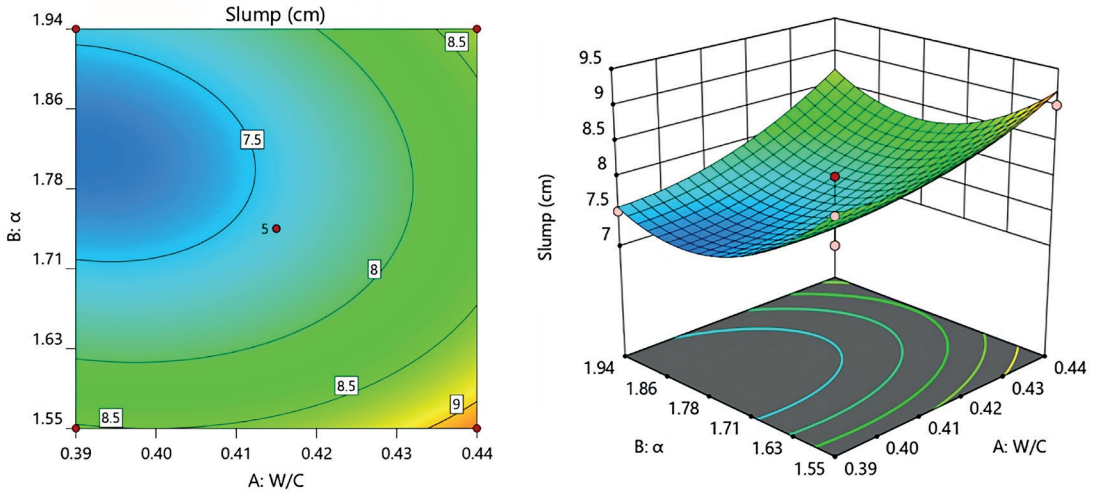

Fig. 11 Contour lines and 3D surface graphs for a slump

Table 13 ANOVA on the effect of W/C and α using a quadratic response surface model for slump and compressive strength

Source	*Df*	Slump				Compressive strength			
		Sum of squares	F-value	P-value	Estimate	Sum of squares	F- value	P-value	Estimate
Model	5	5.82	9.32	0.0053		170.97	23.95	0.0003	
A-W/C	1	1.64	13.13	0.0085	0.4527	35.83	25.1	0.0015	-2.12
B-*α*	1	1.06	8.5	0.0225	-0.3643	14.23	9.97	0.016	1.33
AB	1	0.0625	0.5005	0.5022	0.125	0.0025	0.0018	0.9678	-0.025
A^2	1	0.4793	3.84	0.0909	0.2625	26.11	18.29	0.0037	-1.94
B^2	1	2.83	22.64	0.0021	0.6375	106.49	74.6	< 0.0001	-3.91
Residual	7	0.8742				9.99			
Lack of fit	3	0.1742	0.3318	0.8042		6.09	2.08	0.2452	
Pure error	4	0.7				3.9			
R^2		0.8694				0.9448			
Adj-R^2		0.7761				0.9053			
Predicted R^2		0.6515				0.7269			

Except for W/C*α, all other variables influenced compressive strength. Concrete strength depends on the ratio W/C and α. The sensitivity of compressive strength change depends on the ratio W/C and α according to the linear model but also in combination with nonlinearity (power 2). It found that if the ratio W/C or $(W/C)^2$ increased, the compressive strength decreased; however, the effect of W/C was more efficient than that of $(W/C)^2$. An increase in the ratio of α increases the compressive strength of concrete; for the quadratic form, α^2 reduces the compressive strength, in which the effect of quadratic α^2 was more efficient than that of first-order α. Each unit reduction in W/C resulted in an average decrease of 2.12 in compressive strength. With each increase in α, the compressive strength increased by 1.33 but decreased by 3.91 in the quadratic form. As the W/C ratio reduces, there is an increase in concrete strength, indicating a substantial impact of the W/C ratio on the strength of concrete. Moreover, it is crucial to note that an improper selection of the α ratio can lead to a high degree of workability in the concrete mixture and decrease compressive strength. Fig. 12 shows a 3D surface and contour plot of the compressive strength.

Table 14 presents the ANOVA for the flexural strength response model, considering that for the model, the P-value of "lack of fit" is 0.0006 which is less than the F-value of the model which is 19.45, showing that the model is significant. The R^2 value of 0.9328 is close to the adjusted R^2 value of 0.8849, which confirms a good agreement between the experimental values and the model. P-values less than 0.05 indicates terms of the model are significant. In this case, W/C, α, $(W/C)^2$, and α^2 are meaning terms of the model. The coding equation for flexural strength, Eq. (11):

$$R_3 = 3.54 - 0.2061A + 0.1707B - 0.245A^2 - 0.395B^2 . \quad (11)$$

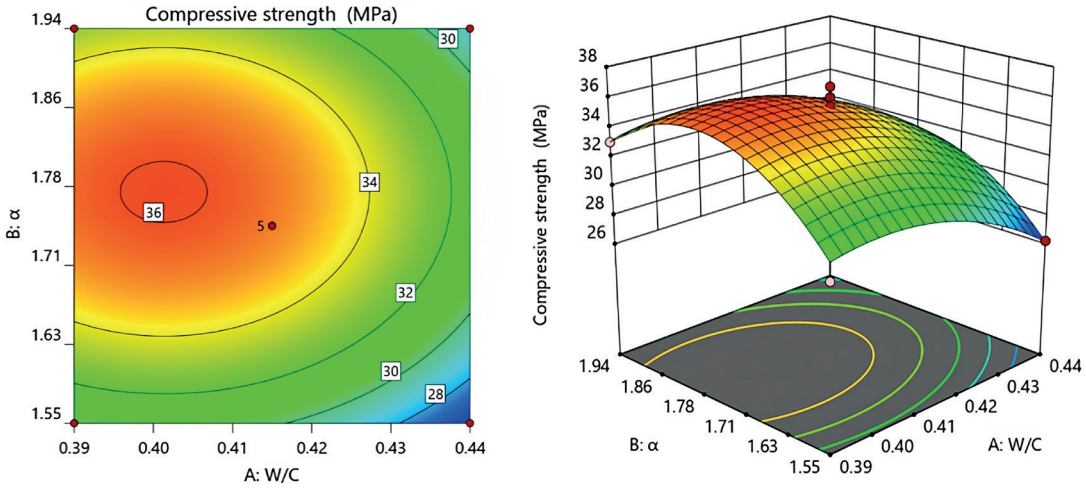

Fig. 12 Contour 3D surface graphs and for compressive strength

Table 14 ANOVA on the effect of W/C and α using a quadratic response surface model for flexural strength and elastic modulus

Source	*Df*	Flexural strength				Elastic modulus			
		Sum of squares	F-value	P-value	Estimate	Sum of squares	F- value	P-value	Estimate
Model	5	0.3866	19.45	0.0006		152.25	12.04	0.0025	
A-W/C	1	0.3397	17.09	0.0044	-0.2061	61.85	24.45	0.0017	-2.78
B-α	1	0.2331	11.73	0.0111	0.1707	15.18	6	0.0441	1.38
AB	1	0.01	0.503	0.5011	-0.05	2.52	0.9976	0.3511	0.7943
A^2	1	0.4176	21	0.0025	-0.245	20.09	7.94	0.0258	-1.7
B^2	1	1.09	54.6	0.0002	-0.395	60.46	23.91	0.0018	-2.95
Residual	7	0.0199				17.7			
Lack of fit	3	0.0091	0.3233	0.8097		2.26	0.1948	0.8949	
Pure error	4	0.028				15.45			
R^2		0.9328				0.8958			
Adj-R^2		0.8849				0.8214			
Predicted R^2		0.8224				0.7635			

Eq. (11) shows that the flexural strength depends on the ratio W/C and the ratio α; the ratio W/C decreases, and the flexural strength of concrete increases. It found that each increase of W/C unit in the first-order form resulted in an average decrease of 0.2061 in flexural strength. Each rise in W/C unit in the quadratic form resulted in an average reduction of 0.245. The quadratic form had 1.19 times the influence of the first-order form on the model. For each increase of α in the first-order form, the mean flexural strength increased by 0.1707 but decreased by 0.395 in the quadratic form. In addition, the synergistic effect of each W/C*α unit reduced the mean flexural strength by 0.05.

The ratio α is too small or too large and has tended to reduce the strength of concrete, which can give reasons as follows: When the amount of fine aggregate was little, the coarse aggregate content was bulky, and the volume of cement mortar was not enough to perform the function of filling and lubricating between coarse aggregate particles. With the same compaction mode, the poor workability of concrete was the cause of the deterioration of the solid structure of the concrete, which resulted in a decrease in the strength of the concrete. An increase in the mass of fine aggregate can cause the coarse aggregate particles to push apart, leading to enhanced workability but reduced strength. Fig. 13 shows a 3D surface and contour plot of the flexural strength.

As shown in Table 14, the P-value of the "lack of fit" is 0.0025 (F-value is 12.04), which shows that the "lack of fit" is not significant compared to the pure error. R^2 of 0.8958 is close to adjusted R^2 of 0.8214, which confirms a suitable fit for the experimental data. The P-values of W/A, α, $(W/C)^2$, and α^2 are less than 0.0500, indicating that these variables have influenced the model. Fig. 14 shows the contour and 3D surface plots of the elastic modulus. The model for the elastic modulus, Eq. (12):

$$R_4 = 34.16 - 2.78A + 1.38B - 1.7A^2 - 2.95B^2 . \quad (12)$$

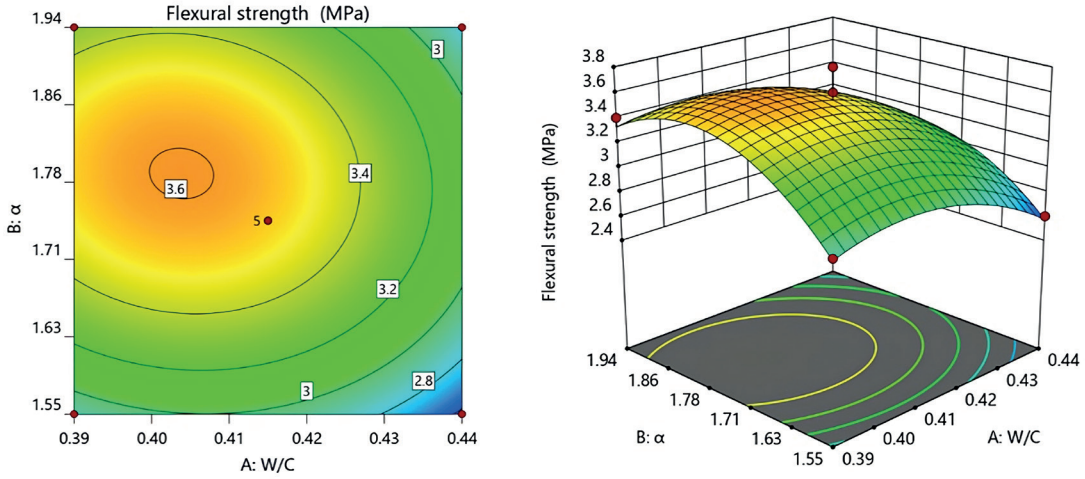

Fig. 13 Surface graphs flexural strength

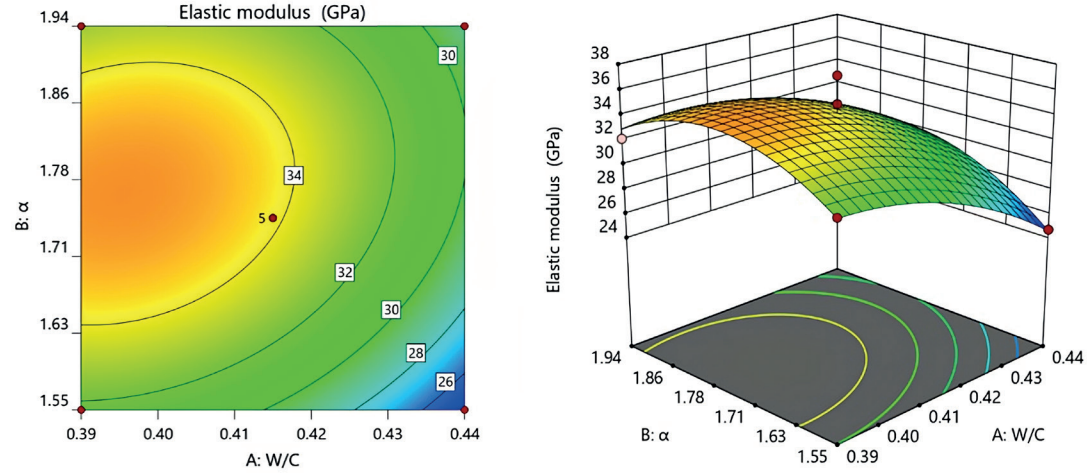

Fig. 14 Lines graphs and for elastic modulus

From Eq. (9)–(12), it has been seen that the W/C ratio is already one of the value factors that significantly affect the elastic modulus and strength of concrete, which is also consistent with previous studies [4]. The effect of the W/C ratio on the strength of concrete was significant; in addition, the selection of an inappropriate α effortlessly crumbled the concrete mixture, reducing its strength property.

3.2 Optimal conditions and verification of the mix design based on engineering properties of concrete

In the optimization process, it is essential to consider all the responses simultaneously to determine the optimal mixture proportion of concrete that meets the requirements for all the studied targets. In the influence of responses, it becomes essential to identify the optimal level that meets all the studied targets [44]. Fig. 15 presented the predicted R_1, R_2, R_3, and R_4 at the optimal ratio W/C of 0.40 and α of 1.78.

The interaction between the two factors W/C and α shows that the sensitivity of changing the strength of concrete depends on the W/C and α, and this was a model obtained in the presence of a good interaction between independent variables (influencing factors) [45]. Table 15 presents the composition of each material for one cubic meter of concrete, which was the optimization of the combination of particle sizes, W/C ratio, and α. These optimized parameters can exploit for subsequent studies. The prediction and experimental results of the engineering properties of concrete based on optimizing the composition of materials are presented in Table 16. The absolute relative percent error (ARPE) of the RSM compared with the obtained laboratory test results was low. ARPE has been calculated according to Eq. (13) [46].

$$ARPE = \left(1 - \frac{Predicted}{Testing}\right) \times 100 \tag{13}$$

Fig. 16 illustrates the careful execution of strength tests conducted on the concrete samples. ARPE of the slump, compressive strength, flexural strength, and elastic modulus were 12.9%, 8.0%, 13.9%, and 14.2%, respectively, and less than 15%. Hence, the model predicting the responses has good accuracy.

4 Conclusions

In this study, natural gravel and waste rock extracted in the Northwest region of Vietnam can utilize as replacements for coarse aggregate (mountain rock) and fine aggregate (river sand) in the production of cement concrete. For predicting the engineering properties of concrete containing gravel and

Table 15 Optimal material composition for one cubic meter of concrete

Cement, kg	Gravel, kg	Waste rock, kg						W/C	α
	19-9.5	9.5-4.75	4.75-2.36	2.36-1.18	1.18-0.6	0.6-0.3	0.3-0.15		
450	722	453	146	77	109	137	185	0.40	1.78

Table 16 Predictive and experimental results

Parameter	Goal	Predicted value	Testing value	Unit
A	In range	0.40	-	
B	In range	1.78	-	
R_1	None	7.4	8.5 (0.5)[a]	cm
R_2	Maximum	36.1	33.2 (3.68)	MPa
R_3	Maximum	3.6	3.1 (1.18)	MPa
R_4	Maximum	35.3	30.6 (3.43)	GPa

[a] The value in () is the value representing the standard deviation.

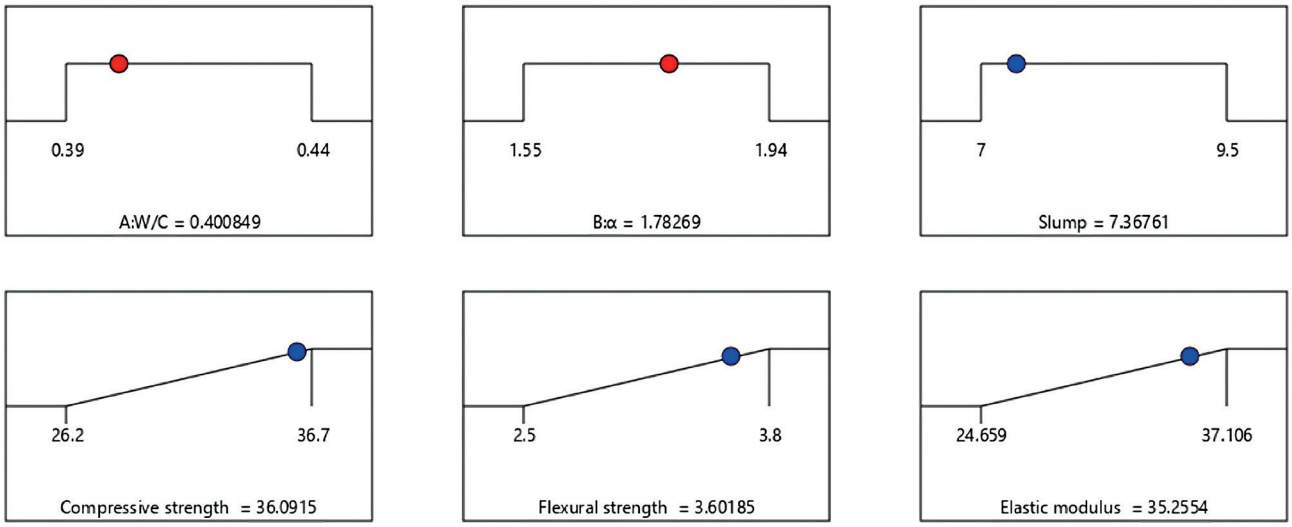

Fig. 15 Optimization of variables and results

waste rock, a component design method based on the optimal distribution (arrangement) of aggregate particles by size with a response surface methodology has been proposed.

The statistical error analysis used to evaluate the RSM model shows that the quadratic polynomial model can find a suitable for describing and predicting the slump of fresh concrete mixture, compressive, flexural strength, and elastic modulus of cured concrete. Caused of its high predictive performance, the RSM model was well suited to predict the engineering properties of concrete, therefore saving time on laboratory experiments. This study can use to select the appropriate mixtures proportion of gravel and waste rock-contained concrete with required compressive strength from 30 MPa to 35 MPa, a combination of the dense packing method and RSM.

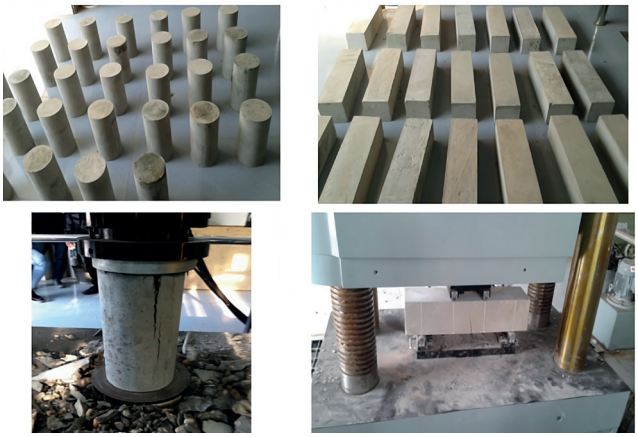

Fig. 16 Experiment to determine mechanical properties of concrete samples

References

[1] Danielsen, S. W., Kuznetsova, E. "Environmental impact and sustainability in aggregate production and use", Engineering Geology for Society and Territory, 5, pp. 41–44, 2015. https://doi.org/10.1007/978-3-319-09048-1_7

[2] Quiroga, P. N., Fowler, D. W. "The effect of the aggregates characteristics on the performance of Portland cement concrete", The University of Texas at Austin, Austin, TX, USA, Rep. ICAR 104-1F, 2003.

[3] Woode, A., Amoah, D. K., Aguba, I. A., Ballow, P. "The effect of maximum coarse aggregate size on the compressive strength of concrete produced in Ghana", Civil and Environmental Research, 7(5), pp. 7–12, 2015.

[4] Neville, A. M. "Properties of concrete", Longman, 1995. ISBN: 0-582-23070-5

[5] Aginam, C. H., Chidolue, C. A., Nwakire, C. "Investigating the effects of coarse aggregate types on the compressive strength of concrete", International Journal of Engineering Research and Applications, 3(4), pp. 1140–1144, 2013.

[6] Saxena, S., Pofale, A. D. "Effective utilization of fly ash and waste gravel in green concrete by replacing natural sand and crushed coarse aggregate", Materials Today: Proceedings, 4(9), pp. 9777–9783, 2017. https://doi.org/10.1016/j.matpr.2017.06.266

[7] Brady, G. S., Clauser, H. H., Vaccari, J. A. "Materials handbook: an encyclopedia for managers, technical professionals, purchasing and production managers, technicians, and supervisors", McGraw-Hill, 2002. ISBN: 9780071360760

[8] Al-Majeed, I., Al-Khafaji, F. F., Al-Saeedi, A. A. "Investigating the effect of different forms of gravel as an aggregate on compressive strength of concrete", International Journal of Advances in Mechanical and Civil Engineering, 5(2), pp. 41–45, 2018.

[9] Sulymon, N., Ofuyatan, O., Adeoye, O., Olawale, S., Busari, A., Bamigboye, G., Jolayemi, J. "Engineering properties of concrete made from gravels obtained in Southwestern Nigeria", Cogent Engineering, 4(1), 1295793, 2017. https://doi.org/10.1080/23311916.2017.1295793

[10] Karakaş, A., Smith, MR., Collis, L. "M. R. Smith and L. Collis (eds): Aggregates: sand, gravel, and crushed rock aggregates for construction purposes (3rd edition)", Arabian Journal of Geosciences, 13, 11, 2020. https://doi.org/10.1007/s12517-019-4975-y

[11] Mamirov, M., Hu, J., Kim, Y.-R. "Effective Reduction of Cement Content in Pavement Concrete Mixtures Based on Theoretical and Experimental Particle Packing Methods", Journal of Materials in Civil Engineering, 33(10), 04021277, 2021. https://doi.org/10.1061/(ASCE)MT.1943-5533.0003890

[12] Shen, W., Liu, Y., Cao, L., Huo, X., Yang, Z., Zhou, C., He, P., Lu, Z. "Mixing design and microstructure of ultra high strength concrete with manufactured sand", Construction and Building Materials, 143, pp. 312–321, 2017. https://doi.org/10.1016/j.conbuildmat.2017.03.092

[13] Nanthagopalan, P., Santhanam, M. "Fresh and hardened properties of self-compacting concrete produced with manufactured sand", Cement and Concrete Composites, 33(3), pp. 353–358, 2011. https://doi.org/10.1016/j.cemconcomp.2010.11.005

[14] Shen, W., Yang, Z., Cao, L., Cao, L., Liu, Y., Yang, H., Lu, Z., Bai, J. "Characterization of manufactured sand: Particle shape, surface texture and behavior in concrete", Construction and Building Materials, 114, pp. 595–601, 2016. https://doi.org/10.1016/j.conbuildmat.2016.03.201

[15] Goncalves, J. P., Tavares, L. M., Toledo Filho, R. D., Fairbairn, E. M. R., Cunha, E. R. "Comparison of natural and manufactured fine aggregates in cement mortars", Cement and Concrete Research, 37(6), pp. 924–932, 2007. https://doi.org/10.1016/j.cemconres.2007.03.009

[16] Binici, H., Aksogan, O. "Durability of concrete made with natural granular granite, silica sand and powders of waste marble and basalt as fine aggregate", Journal of Building Engineering, 19, pp. 109–121, 2018. https://doi.org/10.1016/j.jobe.2018.04.022

[17] Cox, D. R., Reid, N. "The theory of the design of experiments", CRC Press, 2000. ISBN: 9780429126284 https://doi.org/10.1201/9781420035834

[18] Dean, A., Morris, M., Stufken, J., Bingham, D. "Handbook of design and analysis of experiments", CRC Press, 2015. ISBN: 9780429096341
https://doi.org/10.1201/b18619

[19] Mohammed, B. S., Khed, V. C., Nuruddin, M. F. "Rubbercrete mixture optimization using response surface methodology", Journal of Cleaner Production, 171, pp. 1605–1621, 2018.
https://doi.org/10.1016/j.jclepro.2017.10.102

[20] Alyamac, K. E., Ghafari, E., Ince, R. "Development of eco-efficient self-compacting concrete with waste marble powder using the response surface method", Journal of Cleaner Production, 144, pp. 192–202, 2017.
https://doi.org/10.1016/j.jclepro.2016.12.156

[21] Hou, D., Chen, D., Wang, X., Wu, D., Ma, H., Hu, X., Zhang, Y., Wang, P., Yu, R. "RSM-based modelling and optimization of magnesium phosphate cement-based rapid-repair materials", Construction and Building Materials, 263, 120190, 2020.
https://doi.org/10.1016/j.conbuildmat.2020.120190

[22] Aziminezhad, M., Mahdikhani, M., Memarpour, M. M. "RSM based modeling and optimization of self-consolidating mortar to predict acceptable ranges of rheological properties", Construction and Building Materials, 189, pp. 1200–1213, 2018.
https://doi.org/10.1016/j.conbuildmat.2018.09.019

[23] Habibi, A., Ramezanianpour, A. M., Mahdikhani, M. "RSM-based optimized mix design of recycled aggregate concrete containing supplementary cementitious materials based on waste generation and global warming potential", Resources, Conservation and Recycling, 167, 105420, 2021.
https://doi.org/10.1016/j.resconrec.2021.105420

[24] ASTM "ASTM C188-17(2023) Standard Test Method for Density of Hydraulic Cement", ASTM International, West Conshohocken, PA, USA, 2023.
https://doi.org/10.1520/C0188-17R23

[25] ASTM "ASTM C187-16 Standard Test Method for Amount of Water Required for Normal Consistency of Hydraulic Cement Paste", ASTM International, West Conshohocken, PA, USA, 2023.
https://doi.org/10.1520/C0187-16

[26] ASTM "ASTM C204-18e1 Standard Test Methods for Fineness of Hydraulic Cement by Air-Permeability Apparatus", ASTM International, West Conshohocken, PA, USA, 2023.
https://doi.org/10.1520/C0204-18E01

[27] ASTM "ASTM C191-21 Standard Test Methods for Time of Setting of Hydraulic Cement by Vicat Needle", ASTM International, West Conshohocken, PA, USA, 2021.
https://doi.org/10.1520/C0191-21

[28] ASTM "ASTM C109/C109M-20 Standard Test Method for Compressive Strength of Hydraulic Cement Mortars (Using 2-in. or [50-mm] Cube Specimens)", ASTM International, West Conshohocken, PA, USA, 2020.
https://doi.org/10.1520/C0109_C0109M-20

[29] ASTM "ASTM C136-06 Standard Test Method for Sieve Analysis of Fine and Coarse Aggregates", ASTM International, West Conshohocken, PA, USA, 2015.
https://doi.org/10.1520/C0136-06

[30] ASTM "ASTM C127-15 Standard Test Method for Relative Density (Specific Gravity) and Absorption of Coarse Aggregate", ASTM International, West Conshohocken, PA, USA, 2016.
https://doi.org/10.1520/C0127-15

[31] ASTM "ASTM C128-01 Standard Test Method for Relative Density (Specific Gravity) and Absorption of Fine Aggregate", ASTM International, West Conshohocken, PA, USA, 2017.
https://doi.org/10.1520/C0128-01

[32] ASTM "ASTM C29/C29M-07 Standard Test Method for Bulk Density ('Unit Weight') and Voids in Aggregate", ASTM International, West Conshohocken, PA, USA, 2010.
https://doi.org/10.1520/C0029_C0029M-07

[33] ASTM "ASTM C131/C131M-20 Standard Test Method for Resistance to Degradation of Small- Size Coarse Aggregate by Abrasion and Impact in the Los Angeles Machine", ASTM International, West Conshohocken, PA, USA, 2020.
https://doi.org/10.1520/C0131_C0131M-20

[34] ASTM "ASTM D6928-17 Standard Test Method for Resistance of Coarse Aggregate to Degradation by Abrasion in the Micro-Deval Apparatus", ASTM International, West Conshohocken, PA, USA, 2017.
https://doi.org/10.1520/D6928-17

[35] ASTM "ASTM C1260-22 Standard Test Method for Potential Alkali Reactivity of Aggregates (Mortar-Bar Method)", ASTM International, West Conshohocken, PA, USA, 2022.
https://doi.org/10.1520/C1260-22

[36] ASTM "ASTM C192/C192M-14 Standard Practice for Making and Curing Concrete Test Specimens in the Laboratory", ASTM International, West Conshohocken, PA, USA, 2015.
https://doi.org/10.1520/C0192_C0192M-14

[37] ASTM "ASTM C143/C143M-12 Standard Test Method for Slump of Hydraulic-Cement Concrete", ASTM International, West Conshohocken, PA, USA, 2015.
https://doi.org/10.1520/C0143_C0143M-12

[38] ASTM "ASTM C39/C39M-21 Standard Test Method for Compressive Strength of Cylindrical Concrete Specimens", ASTM International, West Conshohocken, PA, USA, 2021.
https://doi.org/10.1520/C0039_C0039M-21

[39] ASTM "ASTM C78/C78M-22 Standard Test Method for Flexural Strength of Concrete (Using Simple Beam with Third-Point Loading)", ASTM International, West Conshohocken, PA, USA, 2022.
https://doi.org/10.1520/C0078_C0078M-22

[40] ASTM "ASTM C469/C469M-14 Standard Test Method for Static Modulus of Elasticity and Poisson's Ratio of Concrete in Compression", ASTM International, West Conshohocken, PA, USA, 2021.
https://doi.org/10.1520/C0469_C0469M-14

[41] Powers, M. C. "A new roundness scale for sedimentary particles", Journal of Sedimentary Research, 23(2), pp. 117–119, 1953.
https://doi.org/10.1306/D4269567-2B26-11D7-8648000102C1865D

[42] ASTM "ASTM C33/C33M-18 Standard Specification for Concrete Aggregates", ASTM International, West Conshohocken, PA, USA, 2018.
https://doi.org/10.1520/C0033_C0033M-18

[43] Jiao, D., Shi, C., Yuan, Q., An, X., Liu, Y. "Mixture design of concrete using simplex centroid design method", Cement and Concrete Composites, 89, pp. 76–88, 2018.
https://doi.org/10.1016/j.cemconcomp.2018.03.001

[44] Oehlert, G. W. "A first course in design and analysis of experiments", W. H. Freeman, 2010. ISBN0-7167-3510-5 [online] Available at: https://www.academia.edu/11316527/A_First_Course_in_Design_and_Analysis_of_Experiments

[45] Nassar, A. I., Thom, N., Parry, T. "Optimizing the mix design of cold bitumen emulsion mixtures using response surface methodology", Construction and Building Materials, 104, pp. 216–229, 2016.
https://doi.org/10.1016/j.conbuildmat.2015.12.073

[46] Pilkington, J. L., Preston, C., Gomes, R. L. "Comparison of response surface methodology (RSM) and artificial neural networks (ANN) towards efficient extraction of artemisinin from Artemisia annua", Industrial Crops and Products, 58, pp. 15–24, 2014.
https://doi.org/10.1016/j.indcrop.2014.03.016